Theoret. Comput. Fluid Dynamics (2004) 18: 27–41
Digital Object Identifier (DOI) 10.1007/s00162-004-0146-0

Theoretical and Computational Fluid Dynamics

Original article

"Perfect" modeling framework for dynamic SGS model testing in large eddy simulation

Giuliano De Stefano[1], Oleg V. Vasilyev[2]

[1] Dipartimento di Ingegneria Aerospaziale e Meccanica, Seconda Universitá di Napoli, 81031 Aversa, Italy
[2] Department of Mechanical Engineering, University of Colorado, 427 UCB, Boulder, CO 80309, USA

Received November 21, 2003 / Accepted June 15, 2004
Published online August 26, 2004
Communicated by T.B. Gatski

Abstract. A *perfect* modeling framework for the systematic study of the effect of filter shape on the resolved scales of motion in large eddy simulation is developed. The effects of the explicit and implicit filtering approaches in large eddy simulation are considered. A simple model for smooth filtering is proposed and the related effects are analyzed. The proposed approach provides an effective research tool for assessing the behavior of sub-grid scale models in a dynamic fashion. The performances of various classical models are examined by using the *perfect* modeling formalism for simulating the large and/or the small residual scales effect. Numerical experiments are performed for decaying isotropic turbulence. The consistency of the sub-grid scale models with the effective composite filter employed in real simulations is discussed. The necessity of using mixed models when solving doubly-filtered Navier–Stokes equations is verified. It is found that time evolution of large scale velocity field is more sensitive to sub-grid large scale models like Bardina model, while the grid-filtered sub-filter scale model is necessary to ensure the proper energy dissipation.

Key words: large eddy simulation, LES, SGS modeling, filtering, dynamic test

1 Introduction

In *large eddy simulation* (LES) of turbulence, one can actually simulate the most energetic, large eddies of the flow, by modeling the effect of the residual ones. The formal scale separation is obtained by means of a low-pass filtering operation, that leads to the definition of *filtered* (or *large-scale*) and *residual* (or *small-scale*) fields. The filtering operation can be implicitly introduced by the numerical discretization of the governing equations (*grid filtering*) or explicitly performed during the simulation (*explicit filtering*). Since the original works on LES (Smagorinsky [27], Deardorff [5], Leonard [16], Schumann [26]), both the finite support of the computational mesh and the low-pass filtering characteristics of the discrete operators (Rogallo and Moin [24], Lund [19]) have been exploited to implicitly filter the Navier–Stokes (NS) equations. In other words, the results of calculations with low resolution have been interpreted as filtered solutions. Only more recently, an explicit filtering operation has been introduced to unambiguously reduce the degrees of

Correspondence to: O.V. Vasilyev (e-mail: Oleg.Vasilyev@Colorado.edu)

freedom of the simulated flow and to control the numerical errors (Lund and Kaltenbach [20], Ghosal [12], Vasilyev et al. [29], Geurts and Frolich [11]). In this case, the mathematical model itself is modified, leading to the definition of the filtered Navier–Stokes (FNS) equations and, at least in principle, the issues of filtering and numerical method are kept separate.

The distinction between the two approaches is rarely considered: they both are usually referred to as LES without taking into account the substantial differences between them. The conceptual mathematical difference becomes evident when looking at the effect of the grid refinement. In FNS simulation, if the filter width is kept constant, the numerical solution tends towards the large-scale field. In fact, the numerical mesh for LES is typically chosen such that, though too coarse to allow a direct numerical simulation (DNS), it is fine enough to resolve large-scale motions. On the contrary, without introducing the explicit filtering, the grid filter width changes with the mesh size and there is no convergence, until the DNS solution is approached for very fine meshes. However, these remain pure conjectures, unless the issue of modeling the unknown residual stresses is considered.

It should be noted that the grid filtering should also be considered even in LES with explicit filtering. Even when the numerical grid is fine enough to solve the *large-scale* motions, the numerical discretization of the governing equations results in additional implicit filtering that can not be ignored, unless a very accurate discretization is employed or a large filter width to grid ratio is used. Thus, the issues of filtering and modeling are independent from the numerical method only from a theoretical point of view and the real LES equations should be considered as the doubly filtered NS equations. In fact, a decomposition of the total residual stress appearing in the LES equations into a term mainly due to discretization and another mainly due to explicit filtering is particularly useful, e.g. (Carati et al. [2]).

The objectives of this paper are manifold: The first concerns the development of the *perfect* modeling approach introduced by De Stefano and Vasilyev [4] as a tool for dynamical testing of sub-grid scale models. The second concerns the understanding of the effect of the superposition of explicit and implicit filtering operations on the dynamics of the resolved large scale structures. Finally, the performances of different commonly used sub-grid scale models are analyzed by partially or fully modeling the effect of the residual field using the *perfect* modeling paradigm. In contrast to a priori analysis of SGS models or a posteriori comparison of the LES and DNS results commonly found in LES literature, the *perfect* modeling framework enables us to analyze the contribution of each separate sub-models in a dynamic fashion. Note that approaches analogous in spirit to *perfect* modeling formalism can be found in (Geurts [10], Domaradzki and Saiki [6], Stoltz and Adams [28]).

The rest of the paper is organized as follows: Sect. 2 briefly describes the main concepts and provides definitions that are used throughout the paper. This section is mainly intended to avoid confusion caused by the multiplicity of definitions available in the LES literature and to prepare the framework for the following discussion. The effect of smooth filtering is examined in Sect. 3, while Sect. 4 focuses on consistency between filtering, modeling procedure and the numerical method. Finally, concluding remarks are drawn in Sect. 5.

2 Filtering in large Eddy simulation

In this paper, we consider incompressible turbulent flow of a Newtonian fluid with constant physical properties, governed by the continuity and NS equations

$$\frac{\partial u_j}{\partial x_j} = 0 \,, \tag{1}$$

$$\frac{\partial u_j}{\partial t} + \frac{\partial u_j u_k}{\partial x_k} = -\frac{\partial p}{\partial x_j} + \nu \frac{\partial^2 u_j}{\partial x_k \partial x_k} \,, \tag{2}$$

where p stands for the reduced pressure and ν for the kinematic viscosity of the fluid. The large-scale field is defined by means of a low-pass filtering operation, that can be carried out either in physical or Fourier space.

Table 1. Summary of filtered velocity definitions

Physical Space	Wavenumber Space	Description
$\boldsymbol{u}$	$\widehat{\boldsymbol{u}}$	unfiltered velocity field
$\bar{\boldsymbol{u}}$	$\widehat{\bar{\boldsymbol{u}}} \equiv \widehat{F}\widehat{\boldsymbol{u}}$	explicitly filtered (large-scale) velocity field
$\boldsymbol{u}' \equiv \boldsymbol{u} - \bar{\boldsymbol{u}}$	$\widehat{\boldsymbol{u}'} \equiv (1-\widehat{F})\widehat{\boldsymbol{u}}$	small-scale residual velocity field
$\widetilde{\boldsymbol{u}}$	$\widehat{\widetilde{\boldsymbol{u}}} \equiv \widehat{G}\widehat{\boldsymbol{u}}$	implicitly filtered velocity field
$\widetilde{\bar{\boldsymbol{u}}}$	$\widehat{\widetilde{\bar{\boldsymbol{u}}}} \equiv \widehat{G}\widehat{\bar{\boldsymbol{u}}} \equiv \widehat{G}\widehat{F}\widehat{\boldsymbol{u}} \equiv \widehat{H}\widehat{\boldsymbol{u}}$	doubly filtered velocity field
$\bar{\boldsymbol{u}}'' \equiv \bar{\boldsymbol{u}} - \widetilde{\bar{\boldsymbol{u}}}$	$\widehat{\bar{\boldsymbol{u}}''} \equiv (1-\widehat{G})\widehat{\bar{\boldsymbol{u}}} \equiv (1-\widehat{G})\widehat{F}\widehat{\boldsymbol{u}}$	large-scale residual velocity field
$\widetilde{\boldsymbol{u}'} \equiv \widetilde{\boldsymbol{u}} - \widetilde{\bar{\boldsymbol{u}}}$	$\widehat{\widetilde{\boldsymbol{u}'}} \equiv \widehat{G}\widehat{\boldsymbol{u}'} \equiv \widehat{G}(1-\widehat{F})\widehat{\boldsymbol{u}}$	filtered small-scale residual velocity field

2.1 Explicit filtering

The desired scale separation is obtained by applying a low-pass spatial filter to the velocity field, or any other turbulent field of interest, according to

$$\bar{\boldsymbol{u}}(\mathbf{x}, t) = \int \mathrm{d}\boldsymbol{\kappa}\, e^{\mathrm{i}\boldsymbol{\kappa}\cdot\mathbf{x}}\, \widehat{F}(\boldsymbol{\kappa})\, \widehat{\boldsymbol{u}}(\boldsymbol{\kappa}, t)\ , \tag{3}$$

where $\boldsymbol{\kappa}$ is the wave number vector, $\mathrm{i}^2 = -1$, $\widehat{F}$ is a suitable filter function, and $\widehat{(\cdot)}$ denotes the Fourier transform. We assume a uniform filter width, such that the filtering operation commutes with spatial differentiation. In this paper, three-dimensional (3-D) filter functions are simply constructed as the tensorial product of 1-D filters acting along each spatial direction, i.e., for uniform filtering, $\widehat{F}(\boldsymbol{\kappa}) \equiv \widehat{F}_1(\kappa_1)\ \widehat{F}_1(\kappa_2)\ \widehat{F}_1(\kappa_3)$. The 1-D filter is parameterized in terms of the characteristic filter wave number κ_F or, equivalently, the characteristic filter width, Δ_F, such that $\kappa_F \Delta_F = \pi$, say $\widehat{F}_1(\kappa; \kappa_F)$. For filters that have zero second moment no consensus on filter width definition exists. For simplicity, we consider the definition given in (Lund [19]), according to which the filter width is determined by the equation $\widehat{F}_1(\kappa_F; \kappa_F) = 0.5$. Note how, throughout this paper, explicitly filtered velocity is denoted by a bar, $\bar{\boldsymbol{u}}$, while the corresponding small-scale residual velocity is denoted by a prime, $\boldsymbol{u}' \equiv \boldsymbol{u} - \bar{\boldsymbol{u}}$. The summary of filtered velocity definitions is given in Table 1.

The evolution equations for the filtered field are the FNS equations, e.g., see (Lund and Kaltenbach [20]):

$$\frac{\partial \bar{u}_j}{\partial t} + \frac{\partial \overline{\bar{u}_j \bar{u}_k}}{\partial x_k} = -\frac{\partial \bar{p}}{\partial x_j} + \nu \frac{\partial^2 \bar{u}_j}{\partial x_k \partial x_k} - \frac{\partial \overline{T}_{jk}}{\partial x_k}, \tag{4}$$

with the incompressibility constrain $\partial \bar{u}_j / \partial x_j = 0$. The residual stresses in Eq. (4),

$$\overline{T}_{jk} = \overline{u_j u_k} - \overline{\bar{u}_j \bar{u}_k}\ , \tag{5}$$

hereafter referred to as *sub-filter scale* (SFS) stresses, take into account the effect of the small scales onto the dynamics of the filtered velocity field. Owing to the fact that the filter shape is a priori prescribed, the non-linear term is explicitly filtered. Indeed, it does not make sense to include into definition (5) the known Leonard stresses $L_{jk}^F = \overline{\bar{u}_j \bar{u}_k} - \bar{u}_j \bar{u}_k$. The terminology *sub-filter scale* stresses is herein used to emphasize that these residual stresses are inherent to the application of the explicit filtering operation, e.g. (Carati et al. [2]). Also, as indicated by the adopted notation, $\overline{T}_{jk}$ can be viewed by itself as a filtered quantity and each term in the equations has the same frequency content. Note that the present SFS stress definition is different from the commonly used one, e.g. (Chow and Moin [3]). In order to close the FNS Eq. (4), a functional relation, $\overline{T}_{jk} \cong \overline{T}_{jk}^{\mathrm{mod}}(\bar{\boldsymbol{u}})$, expressing the SFS stress tensor as a function of the unknown filtered field is needed.

From a physical point of view, one would like to follow the dynamics of flow structures down to a given size, that is to solve the turbulent field up to a given wave number, say κ_F. For this reason, the most natural choice for explicit filtering is the sharp Fourier cutoff at κ_F. In this case, the scale separation is the cleanest possible and one can clearly define the *large-scale* field

$$\bar{\boldsymbol{u}}(\mathbf{x}, t) = \int\limits_{|\kappa_1| \le \kappa_F} \mathrm{d}\kappa_1 \int\limits_{|\kappa_2| \le \kappa_F} \mathrm{d}\kappa_2 \int\limits_{|\kappa_3| \le \kappa_F} \mathrm{d}\kappa_3\, e^{\mathrm{i}\boldsymbol{\kappa}\cdot\mathbf{x}}\, \widehat{\boldsymbol{u}}(\boldsymbol{\kappa}, t)\ . \tag{6}$$

According to definition (5), the SFS stresses do not involve small scale motions, exactly accounting for the effect of the filtered out small scales onto the dynamics of the large ones. On the contrary, for smooth filters, there is an overlapping between large and small scales and the solution of the FNS equations (4) lacks some of the fundamental properties of the original unfiltered field, as demonstrated in (De Stefano and Vasilyev [4]) for Burgers model turbulence. This will be further demonstrated here for three-dimensional isotropic turbulent flow. It is worth noting that in many practical simulations one may not use a sharp cutoff filter. In this case the next best choice is to use a discrete filter as close to sharp cut-off as possible (Vasilyev et al. [29]). However, throughout this paper the sharp Fourier cutoff at κ_F is prescribed as the explicit filter. It is worth stressing that, since most of the models adopted in turbulent flow simulation are based on the scale-invariance properties of high Reynolds number turbulence in the inertial range, e.g. (Meneveau and Katz [21]), the scale separation characteristic wave number κ_F should be chosen in this range.

Finally, observe that, so far, no numerical approximation has been considered and the FNS equations (4) stand for a modified mathematical model to be numerically solved. They are amenable to be discretized at a spatial resolution of order Δ_F, when supplied with a suitable SFS stress model. At this point, the issue of how the unknown boundary conditions for the filtered field could be derived from the physical ones, prescribed for the unfiltered field, would dramatically arise. However, in this paper the issue is not addressed, since homogeneous turbulent flow is considered for the numerical experiments.

2.2 Grid (implicit) filtering

When numerically solving the governing equations, either unfiltered NS or FNS equations, given the low-pass filtering characteristics of the discrete differencing operators, one actually introduces another, *implicit* filtering operation, also referred to as *grid filtering* (Rogallo and Moin [24], Lund [19]). Note that the implicit filter is very different from the explicit filter, since the former is generally unknown, while the latter is explicitly prescribed. Furthermore, the exact definition of the built-in numerical filter, its shape and width, can not be determined, since, in general, each term in the governing equations is acted on by a distinct method-dependent 1-D filter and a single 3-D implicit filter does not exists (Lund [19]). However, for the simplicity of consideration, we assume that the implicit filtering operation can be viewed as the application of a single uniform filter, $\widehat{G}(\boldsymbol{\kappa}) \equiv \widehat{G}_1(\kappa_1)\widehat{G}_1(\kappa_2)\widehat{G}_1(\kappa_3)$, where $G_1(\kappa;\kappa_G)$ is the 1-D grid filter parameterized in terms of the characteristic wave number κ_G. Hereafter grid-filtered quantities are denoted with a tilde (see Table 1). Thus, in the absence of any explicit filtering operation, the LES equations can be viewed as grid filtered NS equations

$$\frac{\partial \widetilde{u}_j}{\partial t} + \frac{\partial \widetilde{\widetilde{u}_j \widetilde{u}_k}}{\partial x_k} = -\frac{\partial \widetilde{p}}{\partial x_j} + \nu \frac{\partial^2 \widetilde{u}_j}{\partial x_k \partial x_k} - \frac{\partial \widetilde{\tau}_{jk}}{\partial x_k}\,, \tag{7}$$

where the residual stresses, $\widetilde{\tau}_{jk} = \widetilde{u_j u_k} - \widetilde{\widetilde{u}_j \widetilde{u}_k}$, is referred to as *sub-grid scale* (SGS) stresses. Note that the grid-filtered non-linear term can be considered recoverable during the simulation. For this reason, the SGS stresses definition does not involve the Leonard stresses, $L^G_{jk} = \widetilde{\widetilde{u}_j \widetilde{u}_k} - \widetilde{u}_j \widetilde{u}_k$. This point is important and it has too often been overlooked in the LES literature.

In order to close the Eq. (7), a suitable model for the SGS stress tensor, $\widetilde{\tau}_{jk} \cong \widetilde{\tau}^{\mathrm{mod}}_{jk}(\widetilde{\boldsymbol{u}})$, must be introduced. In this context, the model must mimic the effect of flow motions that are not resolved by the actual grid.

When considering the numerical solution of the FNS equations (4), a basic requirement is that $\kappa_G \geq \kappa_F$, a requirement that can be trivially met in spectral simulations. The superposition of explicit and implicit filter formally leads to the doubly filtered NS equations:

$$\frac{\partial \widetilde{\bar{u}}_j}{\partial t} + \frac{\partial \widetilde{\widetilde{\bar{u}}_j \bar{u}_k}}{\partial x_k} = -\frac{\partial \widetilde{\bar{p}}}{\partial x_j} + \nu \frac{\partial^2 \widetilde{\bar{u}}_j}{\partial x_k \partial x_k} - \frac{\partial \widetilde{\bar{\tau}}_{jk}}{\partial x_k}\,, \tag{8}$$

with the continuity constrain $\partial \widetilde{\bar{u}}_j / \partial x_j = 0$. In the above equations, the non-linear term is considered acted on by the same composite filter. Indeed, the residual stresses arising from grid filtering

$$\widetilde{\bar{\sigma}}_{jk} = \widetilde{\bar{u}_j \bar{u}_k} - \widetilde{\widetilde{\bar{u}}_j \bar{u}_k} \tag{9}$$

Table 2. Summary of residual stresses definitions

Definition	Description
$\overline{T}_{jk} \equiv \overline{u_j u_k} - \overline{\bar{u}_j \bar{u}_k}$	sub-filter scale (SFS) stresses
$\widetilde{\overline{\sigma}}_{jk} \equiv \widetilde{\overline{\bar{u}_j \bar{u}_k}} - \widetilde{\overline{\tilde{\bar{u}}_j \tilde{\bar{u}}_k}}$	sub-grid large scale (SGLS) stresses
$\widetilde{\overline{T}}_{jk} \equiv \widetilde{\overline{u_j u_k}} - \widetilde{\overline{\bar{u}_j \bar{u}_k}}$	grid filtered sub-filter scale (GFSFS) stresses
$\widetilde{\overline{\tau}}_{jk} \equiv \widetilde{\overline{u_j u_k}} - \widetilde{\overline{\tilde{\bar{u}}_j \tilde{\bar{u}}_k}}$	total residual stresses

have been added to the grid-filtered sub-filter scale stresses

$$\widetilde{\overline{T}}_{jk} \equiv \widetilde{\overline{u_j u_k}} - \widetilde{\overline{\bar{u}_j \bar{u}_k}} \ , \tag{10}$$

leading to the definition of the total residual stresses:

$$\widetilde{\overline{\tau}}_{jk} = \widetilde{\overline{\sigma}}_{jk} + \widetilde{\overline{T}}_{jk} = \widetilde{\overline{u_j u_k}} - \widetilde{\overline{\tilde{\bar{u}}_j \tilde{\bar{u}}_k}} \ . \tag{11}$$

Basically, $\widetilde{\overline{\sigma}}_{jk}$ represents the contribution of the large-scale residual field and can be referred to as *sub-grid large-scale* (SGLS) stress, while $\widetilde{\overline{T}}_{jk}$ represents the effect of the small-scale one. The latter will be referred to as *grid filtered sub-filter scale* (GFSFS) stress. For a summary of residual stresses definitions see Table 2.

Note that equations (8) correspond to the governing equations for the unknown $\tilde{\bar{\boldsymbol{u}}}$, formally obtained by filtering the original equations (2) by means of the composite filter $\widehat{H} \equiv \widehat{G}\widehat{F}$. In order not to alter the resolved large scales range, the characteristic wave number of the composite filter, κ_H, is set to be equal to κ_F, even if, in practice, it could be smaller.

The doubly filtered equations must be interpreted as the actual LES equations and the total residual stresses $\widetilde{\overline{\tau}}_{jk}$ can be still referred to as SGS stresses. Actually, in the present context, this term is not completely exact but, for the sake of clarity, we prefer to maintain the terminology usually adopted in the literature. In this framework, one can think of either modeling the entire term $\widetilde{\overline{\tau}}_{jk}$ or separately consider the SGLS and GFSFS contributions. Again, the model is usually expressed directly in terms of the resolved field, by introducing a functional relation $\widetilde{\overline{\tau}}_{jk} \cong \widetilde{\overline{\tau}}^{\mathrm{mod}}_{jk}(\tilde{\bar{\boldsymbol{u}}})$.

The superposition of explicit and implicit grid filtering makes it possible to solve only for filtered large scales, $\tilde{\bar{\boldsymbol{u}}}$, leaving the residual large scales, $\bar{\boldsymbol{u}}'' = \bar{\boldsymbol{u}} - \tilde{\bar{\boldsymbol{u}}}$, filtered out of the computations (see Table 1). When explicit and implicit grid filtering commute, one can also look at (8) as the governing equations for the filtered velocity field $\tilde{\bar{\boldsymbol{u}}}$. This alternative viewpoint is quite common in works about LES with explicit filtering, wherein an explicit filtering operation is superimposed onto the implicit filtering associated with the LES grid, in order to clean the highest resolved frequencies, contaminated by numerical errors, e.g. (Lund [19]). We here prefer to keep up the original point of view, since it allows one to clearly identify two successive, conceptually different issues: first, reducing the simulated range of scales by low-pass filtering the governing equations and, then, numerically solve them. Also, note that in spectral simulations, under the condition $\kappa_G \geq \kappa_F$, the grid filtering is actually not effective, that is $\widehat{H} \equiv \widehat{F}$ or, equivalently, $\tilde{\bar{\boldsymbol{u}}} \equiv \bar{\boldsymbol{u}}$. Practically, the same ideal condition is also obtained when a sufficiently fine numerical grid, together with a high-order FD method, is exploited for solving the FNS equations. In this case it holds that $\widetilde{\overline{\sigma}}_{jk} \cong 0$ and $\widetilde{\overline{\tau}}_{jk} \cong \widetilde{\overline{T}}_{jk}$, so that only the small scale contribution must be modeled.

3 Filter shape effect

In this section, the effect of the shape of the filter upon the LES solution is discussed. The influence of the effective filter shape on low order flow statistics is examined by performing numerical experiments with de-

caying isotropic turbulence, thus extending the study conducted for Burgers model turbulence in (De Stefano and Vasilyev [4]).

The numerical experiments are performed by using a pseudo-spectral method with de-aliasing (Ruetsch and Maxey [25]). This allows us to have the simulated flow scales, say $|\kappa| \leq \kappa_{\max}$, practically not affected by any numerical error. The time integration is performed by means of the classical Adams–Bashforth/Crank–Nicolson hybrid scheme. Specifically, the explicit Adams–Bashforth procedure is exploited for the non-linear term and the implicit Crank–Nicolson one for the viscous and forcing terms. In order not to alter the spatial accuracy, the time integration step is kept constant during the simulation at a particularly low level, namely $\Delta t = 10^{-3}\tau_{\text{eddy}}$, where τ_{eddy} is the initial eddy-turnover time.

First of all, a DNS solution of the unfiltered NS equations (2) is obtained on a 128^3 grid (i.e., $\kappa_{\max} = 64$). In order to make de-aliasing, according to the 3/2 rule, a 192^3 enlarged grid is however employed for computing non-linear terms. The full de-aliasing is performed in order to separate the numerical and modeling effects. The simulation is conducted by forcing the flow field until an equilibrium stationary state has reached and the inertial range has developed, say at time $t = t_0$. The random forcing scheme of Eswaran and Pope (Eswaran and Pope [8], Eswaran and Pope [7]) is used for simulating forced turbulence. The Reynolds number of the flow, based upon the Taylor microscale, is $Re_\lambda \cong 72$.

To study how the filtering operation affects the NS solution, we carry out the numerical simulation of the filtered equations, both (4) and (8), by using the same pseudo-spectral code. The forcing procedure is now turned off so that decaying turbulence is actually simulated. Preliminarily, a DNS is conducted until the Reynolds number becomes $Re_\lambda \cong 50$, while the energy content of the flow reduces to about fifty percent of the initial value, say at time $t = t_0 + t_{\text{integr}}$, where $t_{\text{integr}} \cong 0.8\,\tau_{\text{eddy}}$. In the following, let us note $\boldsymbol{u}^{\text{DNS}}$ the DNS velocity field. The DNS solution is used as a reference for all the LES results.

The numerical solution of the filtered equations is conducted by initializing the velocity field with the filtered DNS solution. The wave number corresponding to the smallest flow scale that we are interested in is fixed at $\kappa_F = 16$. Both sharp cutoff and smooth grid filters are considered, corresponding to the same characteristic wave number κ_G, with $\kappa_G \geq \kappa_F$.

The unknown residual terms are dynamically evaluated, for both cases, according to the *perfect* modeling procedure introduced in (De Stefano and Vasilyev [4]). It consists in supplying LES with the ideal SGS stresses evaluated upon the reference DNS solution. Namely, the SGS forces are computed according to the definition during the DNS, evaluated on the LES grid and stored at each discrete time-step, for $t_0 \leq t \leq t_0 + t_{\text{integr}}$. As already successfully experienced (De Stefano and Vasilyev [4]), the *perfect* modeling procedure, when joined to good numerics, allows one to examine the pure effect of filtering.

As far as spectral simulations are considered, when a spectral grid with a sufficiently high number of modes is employed, implicit filtering is not effective and the governing equations to be actually solved remain the FNS ones (4). In our numerical experiments, in order not to have the implicit cutoff induced by the actual pseudo-spectral method, we simply consider a computational grid such that $\kappa_{\max} \geq \kappa_F$; namely, we adopt a 32^3 grid (i.e., $\kappa_{\max} = \kappa_F = 16$). The numerical solution of the FNS equations (4) is conducted by supplying the simulation with the perfect SFS stress term,

$$\overline{T}_{jk}^{\text{per}} = \overline{u_j^{\text{DNS}} u_k^{\text{DNS}}} - \overline{u_j^{\text{DNS}}}\;\overline{u_k^{\text{DNS}}}\,. \tag{12}$$

The time evolution of the total large-scale energy, E_{tot}, and energy dissipation, $-\mathrm{d}E_{\text{tot}}/\mathrm{d}t$, for the *perfect* FNS solution has been verified to be practically the same as for the cutoff filtered (truncated) DNS. As to spectral energy distribution, the spectra for *perfect* FNS, (truncated) DNS and no-modeled solutions are reported in Fig. 1 (left) at a given time instant, $t - t_0 = 0.5\,\tau_{\text{eddy}}$. Note that the energy spectra are plotted normalized with respect to the maximum initial energy density for the unfiltered solution. For comparison, the ideal slope of the inertial range, $-5/3$, is also reported. The classical pile-up of energy at highest large-scale wave numbers is evident when no-modeling procedure is adopted, while the *perfect* modeling procedure provides the exact spectral distribution. This result is obvious but necessary to validate the perfect modeling procedure. In practical simulations, if a good SFS model that mimics the unknown energy flux through the cutoff wave number is available, one is able to recover the right large-scale energy evolution. Moreover, the LES solution can retain most of the energy of the flow. In the present case, owing to the adopted primary filter width and the moderate Reynolds number of the flow, the filtered velocity field has been verified to keep a very high fraction of the energy of the flow. However, even if the model provides the right dissipation,

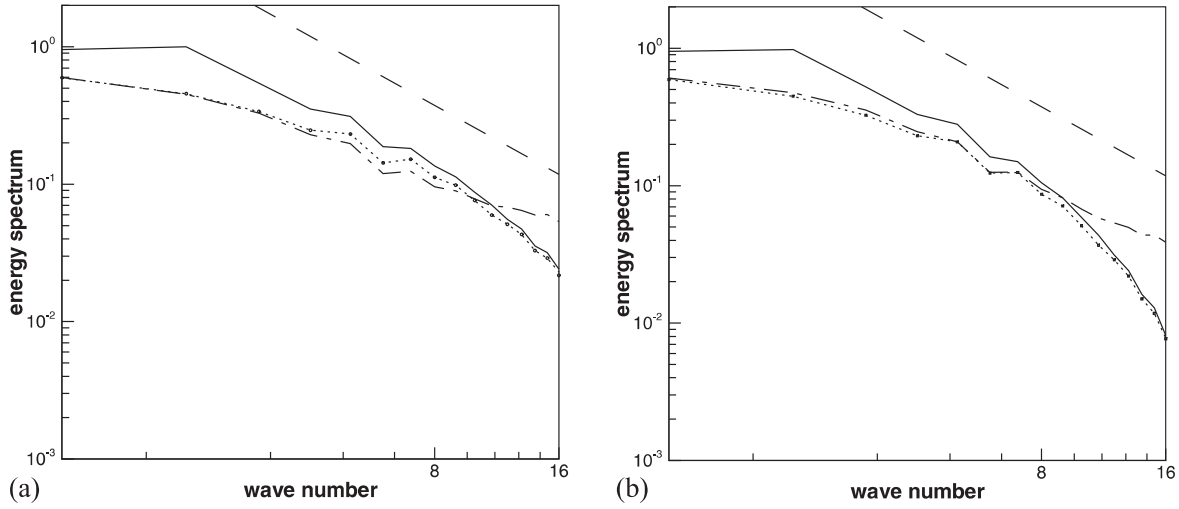

Fig. 1a,b. Density energy spectra for LES with *perfect* SGS models (∘ ∘ ∘) compared to the corresponding filtered DNS (· · · · · ·) and no-model solutions (— · —) for sharp cutoff (left) and smooth filtering (right) cases for $t - t_0 = 0.5\tau_{\text{eddy}}$. The initial filtered DNS spectrum (——) is also shown

the energy spectral distribution in the resolved wave number range could not be well reproduced, as will be shown later.

On the other hand, for low order FD methods, the effect of the superposition of grid filtering can be very strong and must be analyzed with care. However, since the exact definition of the implicit filter can not be known, herein we use a filter that approximates in some sense those involved in real simulations. As an example of a smooth grid filter we consider the truncated top-hat filter, that is, in one spatial dimension

$$\widehat{G}_1(\kappa;\kappa_G) = \begin{cases} \frac{\sin(\pi\kappa/\kappa_0)}{(\pi\kappa/\kappa_0)}, & \text{if } |\kappa| \le \kappa_G \\ 0, & \text{if } |\kappa| > \kappa_G, \end{cases} \tag{13}$$

where $\kappa_0 \equiv \pi\kappa_G/\beta$ stands for the first zero of the transfer function, the coefficient β being such that κ_G effectively stands for the filter characteristic wave number. From imposing $\widehat{G}(\kappa_G;\kappa_G) = 0.5$, it holds $\beta \cong 1.896$. However, this represents only an illustrative example. In fact, as already discussed in Sect. 2, the actual grid filtered equations being solved can not be derived through the simple application of a single filter.

Given the grid filter shape, the residual stress contribution in the LES equations (8) can be perfectly evaluated according to definition (11)

$$\widehat{\tau}_{jk}^{\,\text{per}} = \widehat{u_j^{\text{DNS}} u_k^{\text{DNS}}} - \widehat{u_j^{\text{DNS}}}\,\widehat{u_k^{\text{DNS}}} \quad , \tag{14}$$

where, for sake of simplicity, $\widehat{(\cdot)}$ denotes composite filtering. Thus, ideal LES calculations can be performed starting from the filtered DNS solution, supplied with the perfect model (14). For the present pseudo-spectral simulations, we consider a numerical grid such that $\kappa_{\max} \ge \kappa_G$. For instance, by choosing $\kappa_G = \kappa_F = 16$, a 32^3 grid is adopted. This way, the numerical and the filtering issues are clearly kept apart in our experiments.

Again, as expected, running LES supplied with the perfect SGS stresses, the same energy and energy dissipation evolution of the doubly filtered DNS solution are recovered. Moreover, low order statistics are well captured by perfect LES. For instance, in Fig. 2, the skewness of the derivative of a velocity component is shown. For unfiltered DNS the skewness is nearly constant in time and the value of about -0.5 is in agreement with other studies, e.g., (Meyers et al. [22]). The same good agreement holds for the energy spectra, as illustrated in Fig. 1 (right).

Note how, in the case of composite filtering, even when the LES is conducted with the present ideal SGS model (the best one can imagine) the resolved field loses some important features of the real fully resolved

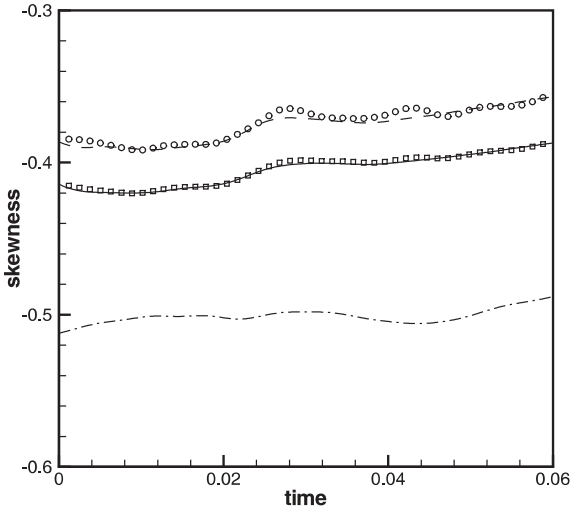

Fig. 2. Skewness of a velocity component derivative for LES with *perfect* models, for sharp cutoff (○ ○ ○) and smooth filtering (□□□), compared to truncated (- - - - - -), double filtered (——) and unfiltered DNS (— · —)

field: for instance, the slope of the energy spectrum in the inertial range is clearly misrepresented (see Fig. 1). Moreover, the LES solution retains less energy with respect to the truncated DNS case, even when $\kappa_G = \kappa_F$. Therefore, the exact reference solution for verifying LES results should be provided by the doubly filtered DNS solution. Unfortunately, in real computations, owing to the filter shape being unknown, it is nearly impossible to make detailed comparisons with filtered DNS or experimental data.

It is worth noting that the LES simulation is usually asked to provide the right large-scale energy spectrum with respect to the truncated DNS. Thus, the SGS model should not only mimic the energy flux through the cutoff wave number, but also remedy the action of smooth filtering onto the large scales.

4 Model consistency

Since the first, pioneering works on the LES approach, e.g., (Piomelli et al. [23]), great attention has been devoted to the issue of consistency between filtering and residual stress modeling. How the SGS model must relate to the actual filter employed is inherent to the residual stresses definition. This is particularly true for LES with explicit filtering, for which the filter function is given and known.

In case of double filtering, the discussion conducted in Sect. 2.2 suggests that one should adopt different models for the different parts of the SGS stress tensor. This leads to the definition of mixed models. In particular, one can attempt to somewhat recover the contribution of the residual large scales in terms of the solved ones, so modeling the SGLS stresses, $\widetilde{\overline{\sigma}}_{jk}$, by approximately inverting the grid filtering operation (Gullbrand and Chow [13], Jeanmart and Winckelmans [14]). As the grid-filter shape is actually unknown, this inversion can be performed only in an approximate way. Along this line, several models have been proposed, starting from the reconstruction model by Leonard [16]. On the other hand, the action of small scale motions essentially resulting in a dissipation, eddy-viscosity models can be exploited for modeling the grid filtered SFS stresses, $\widetilde{T}_{jk}$. Several mixed models can be constructed by combining the above two different methodologies, e.g. (Winckelmans et al. [32]). In this section, after a brief presentation of the various models tested, some numerical results are discussed. The present simulations stand for a sort of dynamic test in which the model is partly evaluated according to the *perfect* modeling formalism.

4.1 SFS and SGS modeling

In order to close the FNS equations (4), a suitable model must be introduced for the unknown SFS stresses (5) We recall that, in this case, the residual stress tensor exactly accounts for the small-scale effect upon the large-scale dynamics. In fact, as expected, by adopting a scale-similarity model, that is by assuming $\boldsymbol{u} \approx \bar{\boldsymbol{u}}$, the model would provide no contribution. The eddy-viscosity Smagorinsky model (Smagorinsky [27]) is

usually adopted for approximating the deviatoric part of the SFS stress tensor,

$$\overline{T}_{jk}^{\,\mathrm{mod}} - \frac{1}{3}\delta_{jk}\overline{T}_{hh}^{\,\mathrm{mod}} = -2C\Delta_F^2\overline{|\overline{\mathbf{S}}|\overline{S}_{jk}}\,, \tag{15}$$

where $|\overline{\mathbf{S}}| \equiv (2\overline{S}_{jk}\overline{S}_{jk})^{1/2}$ and $\overline{S}_{jk}$ stand for the components of the large-scale velocity strain-rate tensor. In our experiments, the coefficient in Eq. (15) is not prescribed a priori but determined, as a function of time, by means of the classical dynamic procedure, e.g., (Germano et al. [9], Lilly [18]). As usual, we fix the test to explicit filter widths ratio at $\alpha = 2$, in order to ensure that the test filter characteristic wave-number still belongs to the inertial range.

Moreover, by considering the LES equations as formally obtained by filtering the NS equations with the composite filter $\widehat{H}$ (explicit sharp cutoff plus smooth grid filter), the SGS stress tensor, $\widehat{\tau}_{jk} \equiv \widehat{u_j u_k} - \widehat{\overline{u}_j}\,\widehat{\overline{u}_k}$, is decomposed into the SGLS term, $\widehat{\sigma}_{jk} \equiv \widehat{\overline{u}_j\overline{u}_k} - \widehat{\overline{u}_j}\,\widehat{\overline{u}_k}$, and the *grid-filtered* SFS one, $\widehat{T}_{jk} \equiv \widehat{u_j u_k} - \widehat{\overline{u}_j\overline{u}_k}$. Hence, the *perfect* modeling approach can be exploited for partly modeling the residual stresses, the remainder being modeled by means of common models. This way, one can address, at least theoretically, the capabilities of different modeling procedures.

The SGLS term can be modeled by means of reconstruction or approximate deconvolution type models, e.g. (Stoltz and Adams [28]). Since the definition of the smooth grid filter is assumed known for the present experiments, by de-convolving the LES field with respect to grid filter, one can obtain the large-scale velocity and directly evaluate the SGLS stresses. The results, not reported here, are exactly equivalent to *perfect* SGLS modeling. In practical simulations, the inversion can be performed only in an approximate way (Gullbrand and Chow [13], Jeanmart and Winckelmans [14], Stoltz and Adams [28]). For instance, if $\boldsymbol{u}^{\mathrm{dec}}$ is the approximate de-convolved velocity, the SGS stress can be approximated as

$$\widehat{\tau}_{jk}^{\,\mathrm{mod}} = \widehat{u_j^{\mathrm{dec}} u_k^{\mathrm{dec}}} - \widehat{\overline{u}_j}\,\widehat{\overline{u}_k}\ . \tag{16}$$

However, due to the unrecoverable loss of information as a result of explicit filtering, it is reasonable to assume that doubly filtered velocity field, $\widehat{\overline{\boldsymbol{u}}}$, can be de-convolved only up to the large scale field, i.e. $\boldsymbol{u}^{\mathrm{dec}} \cong \bar{\boldsymbol{u}}$. Thus, velocity de-convolution, at best, could provide only SGLS stress, since $\overline{\boldsymbol{u}^{\mathrm{dec}}} \cong \boldsymbol{u}^{\mathrm{dec}}$. Alternatively, the SGLS stress can be modeled. In this work two different SGLS models are investigated: the filtered Bardina model (Bardina et al.[1])

$$\widehat{\sigma}_{jk}^{\,\mathrm{mod}} = \widehat{\overline{u}_j}\,\widehat{\overline{u}_k} - \overline{\widehat{\overline{u}_j}\,\widehat{\overline{u}_k}} \tag{17}$$

and the filtered Leonard model (Leonard [17])

$$\widehat{\tau}_{jk}^{\,\mathrm{mod}} = \Delta_H^2\,\overline{\frac{\partial\widehat{\overline{u}}_j}{\partial x_l}\frac{\partial\widehat{\overline{u}}_k}{\partial x_l}}\,. \tag{18}$$

Note that additional explicit filtering is required to ensure the adequate frequency content of the modeled stress. As demonstrated by Winckelmans et al. [31] and confirmed by the results of numerical experiments presented in the following section, this model is able to represent by itself an efficient SGS model. However, the model is not dissipative enough and should be complemented with an additional model that captures the dissipation due to the action of the SFS stresses. Also, the strong link between the Leonard and the Bardina model is well known, e.g. (Winckelmans et al. [32], Winckelmans et al. [31], Vreman et al. [30]). In fact, since most of these models can not reproduce the effect of small-scale turbulence, an explicit dissipation model can be supplied. The eddy-viscosity Smagorinsky model can be adopted for this goal

$$\widehat{T}_{jk}^{\,\mathrm{mod}} - \frac{1}{3}\delta_{jk}\widehat{T}_{hh}^{\,\mathrm{mod}} = -2C\Delta_H^2\overline{|\widehat{\mathbf{S}}|\widehat{S}_{jk}}, \tag{19}$$

where $\widehat{S}_{jk}$ stands for the doubly filtered velocity strain-rate tensor. Again, the overbar at the r.h.s. takes into account how, by definition, the LES solution does not have small-scale components. The model coefficient

can be dynamically determined by introducing a further test cutoff filter at $\alpha\kappa_F$ and consistently defining the doubly test filtered velocity. Note that the resulting dynamic procedure is slightly different from the one used in (Winckelmans et al. [32], Germano et al. [9], Lilly [18]), owing to the difference in grid filtered SFS stress definition (10).

4.2 Numerical experiments

The results of the numerical solution of the FNS equations (4) supplied with the dynamic Smagorinsky SFS model are reported in Fig. 3 in terms of time evolution of total energy and energy dissipation. All the data are normalized with respect to the initial large-scale values. As well known, the dynamic model works very well for sharp cutoff filtering. In fact, as it was demonstrated by Jimenez [15], the dynamic procedure provides a feedback to guarantee the adequate dissipation for the residual scales model. After an initial transient, the dissipation provided by the dynamic model mimics well the ideal one. However, when considering the energy spectrum (see Fig. 4) it is clearly seen that the slope of the inertial range is misrepresented.

As far as SGS modeling for LES equations (8) is concerned, results are obtained by supplying the numerical simulation with various mixed models, obtained by differently combining SGLS and GFSFS models. In

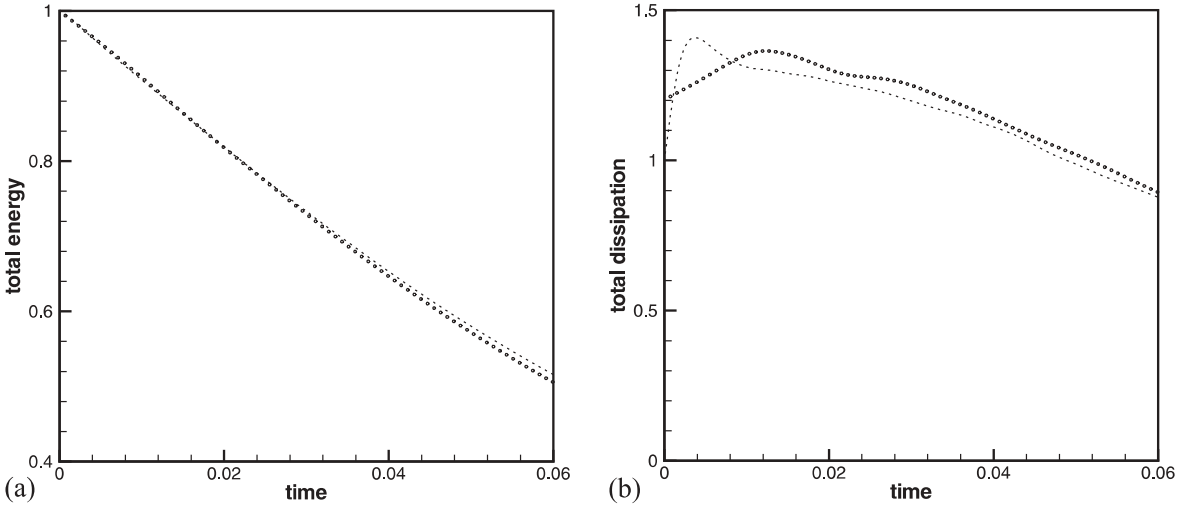

Fig. 3a,b. Temporal evolution of the total large-scale energy (left), E_{tot}, and the energy dissipation (right), $-\mathrm{d}E_{\mathrm{tot}}/\mathrm{d}t$, for the FNS solution with the dynamic SFS model (○ ○ ○) compared to the cutoff filtered DNS (· · · · · ·)

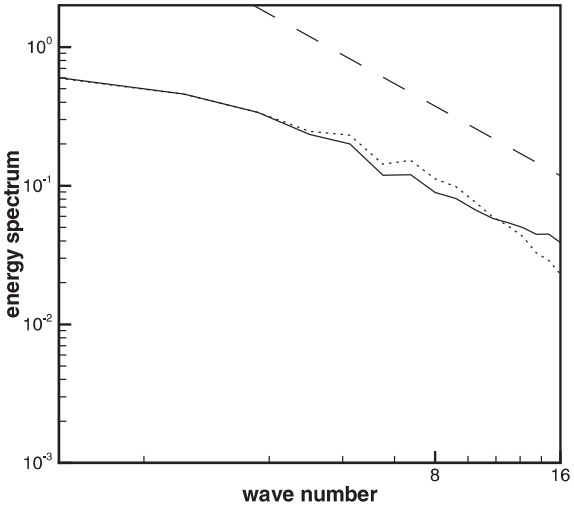

Fig. 4. Density energy spectrum for the FNS solution with the dynamic SFS model (——) compared to the cutoff filtered DNS (· · · · · ·) for $t - t_0 = 0.5\tau_{\mathrm{eddy}}$

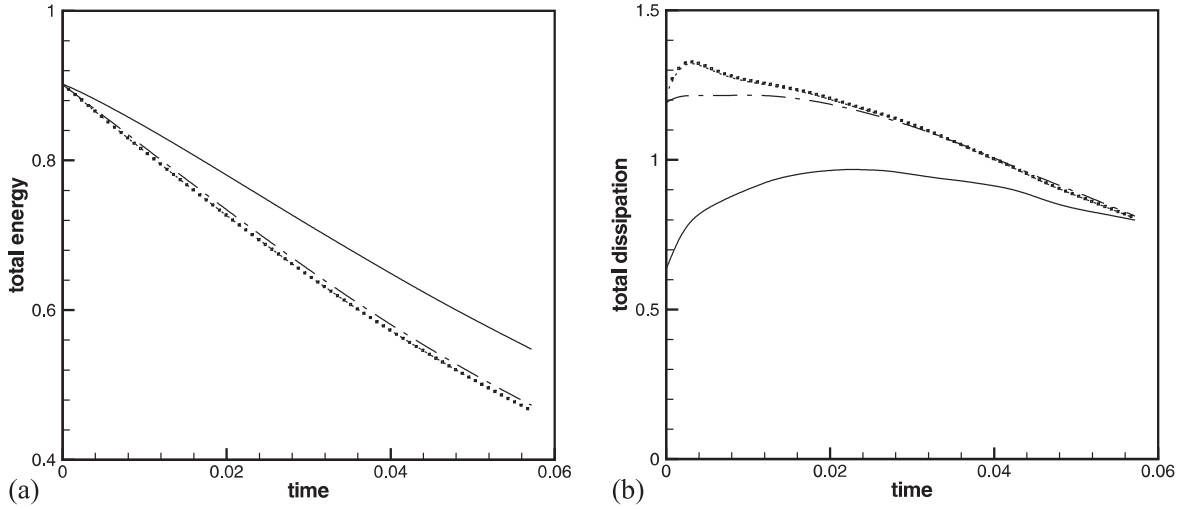

Fig. 5a,b. Temporal evolution of the total resolved large-scale energy (left), $E_{r,\mathrm{tot}}$, and energy dissipation (right), $-\mathrm{d}E_{r,\mathrm{tot}}/\mathrm{d}t$, for the LES solutions with different modeling procedures: *perfect* SGLS with no GFSFS (— · —), no SGLS with *perfect* GFSFS (——), and *perfect* total stress (∘ ∘ ∘) compared to the doubly filtered DNS (· · · · · ·)

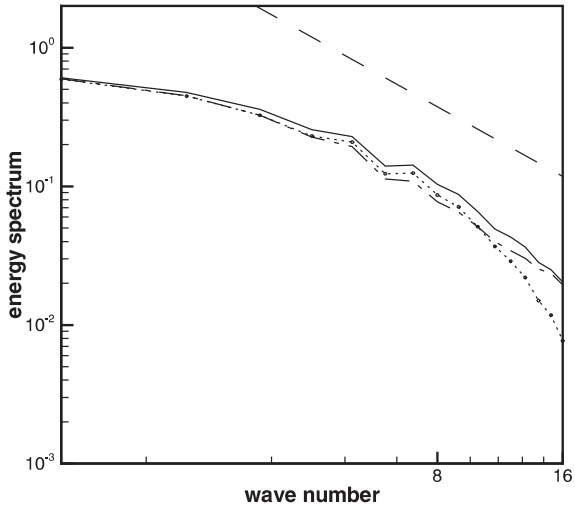

Fig. 6. Density energy spectra for the LES solutions with different models: *perfect* SGLS with no GFSFS (— · —), no SGLS with *perfect* GFSFS (——), and *perfect* total stress (∘ ∘ ∘) compared to the doubly filtered DNS (· · · · · ·) for $t - t_0 = 0.5\tau_{\mathrm{eddy}}$

Fig. 5, the total resolved energy decay and energy dissipation evolution are reported for the following cases: no SGLS modeling with *perfect* GFSFS modeling, *perfect* SGLS modeling with no GFSFS modeling, and *perfect* (total) SGS modeling. By making a comparison with the ideal doubly filtered DNS solution, it appears evident how the model is more sensitive to the large-scale contribution: not modeling SGLS stresses results in a considerably worse solution than the one obtained without GFSFS model, as clearly demonstrated in Fig. 6. This greater sensitivity to large scale contribution is partially due to the de-correlation between the LES and DNS fields. Also, note the energy pile-up at high frequencies when no GFSFS is supplied, which confirms the inadequacy of energy dissipation provided by the perfect SGLS model.

In Fig. 7, the results corresponding to the filtered Bardina model (17) with and without the dynamic Smagorinsky GFSFS model are reported. It is evident how the addition of an eddy-viscosity model is necessary to obtain good LES results. The effect of adding an eddy-viscosity term is less important when using the Leonard modeling procedure (18), for which quite good results are obtained even with no GFSFS model, as illustrated in Fig. 8. However, this result could depend upon the actual flow simulation parameters, for which the GFSFS model is not very important. In fact, by looking at the fraction of energy dissipation provided by the modeled GFSFS stress reported in Fig. 9, it is evident how, owing to the moderate *Re* number of the flow, as well as to the adopted primary filter width, the magnitude of the GFSFS dissipation is smaller than the

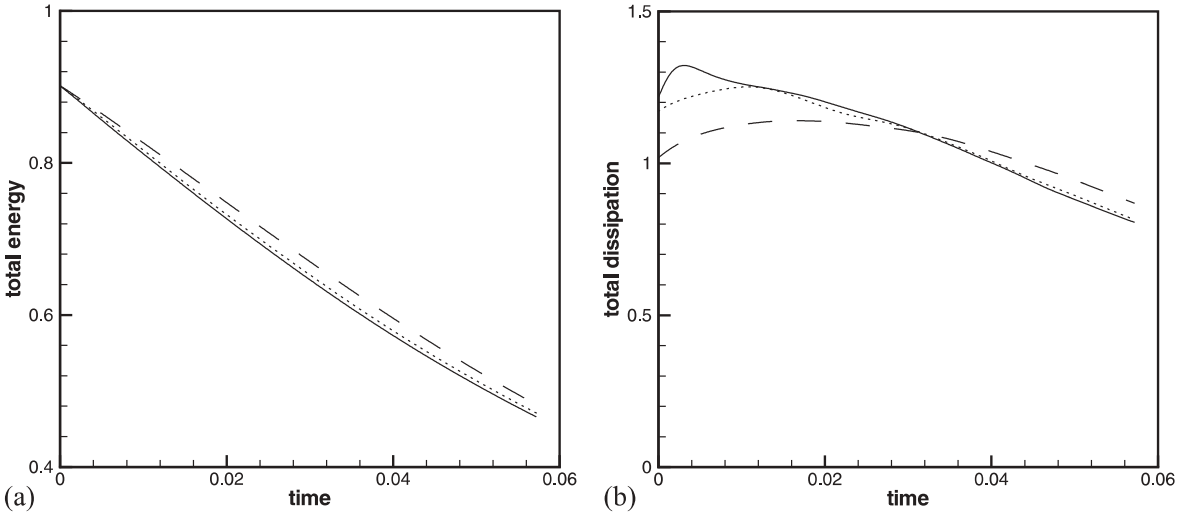

Fig. 7a,b. Temporal evolution of total resolved large-scale energy (left), $E_{r,\mathrm{tot}}$, and energy dissipation (right), $-\mathrm{d}E_{r,\mathrm{tot}}/\mathrm{d}t$, for the LES solutions with filtered *Bardina* model with (· · · · · ·) and without (- - - - - -) the Smagorinsky dynamic model compared to the doubly filtered DNS (——)

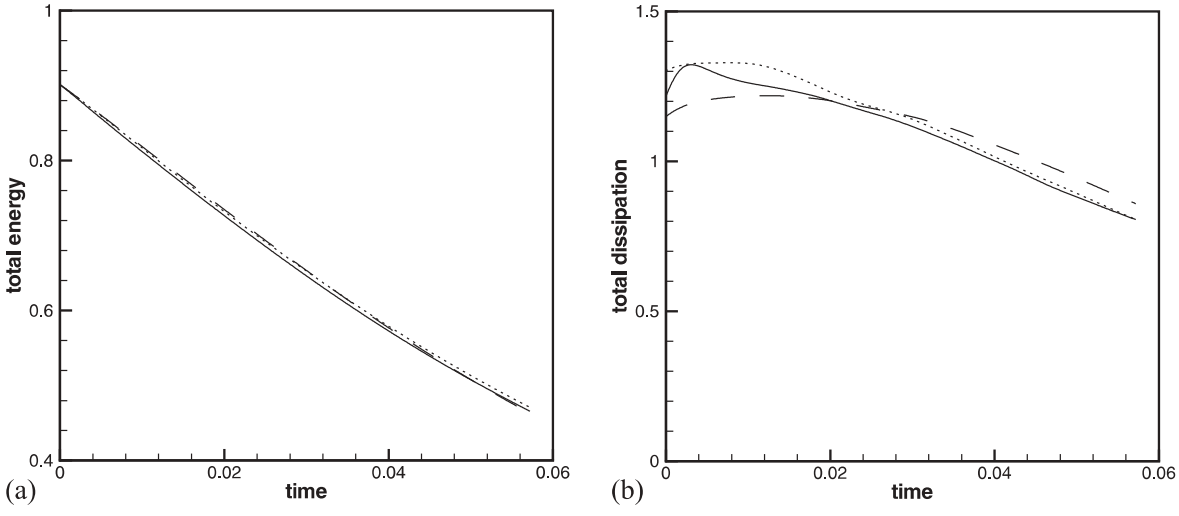

Fig. 8a,b. Temporal evolution of the total resolved large-scale energy (left), $E_{r,\mathrm{tot}}$, and the energy dissipation (right), $-\mathrm{d}E_{r,\mathrm{tot}}/\mathrm{d}t$, for the LES solutions with filtered *Leonard* model with (· · · · · ·) and without (- - - - - -) Smagorinsky dynamic model compared to the doubly filtered DNS (——)

viscous one. For higher filter widths, as well as for higher *Re* number flows, as typical in practical flow simulations, the GFSFS dissipation is expected to be more important. The higher Reynolds number simulations will be conducted in the future.

Finally, further insight can be obtained by examining the energy spectra corresponding to different simulations reported in Fig. 10. It is important to note that, regardless of the adopted SGLS model, the Smagorinsky model provides the wrong slope for the inertial range in the neighborhood of the cutoff frequency when compared to the doubly filtered DNS solution, since it does not capture the additional damping of energy at high frequencies due to the action of smooth filtering. In fact, the Leonard model (18) when used together with the *perfect* grid-filtered SFS model results in the right energy spectrum. However, the Smagorinsky model gives quite good slope when compared to the sharp-cutoff filtered DNS solution. Thus, one needs to be careful when comparing LES results with filtered DNS or experimental results.

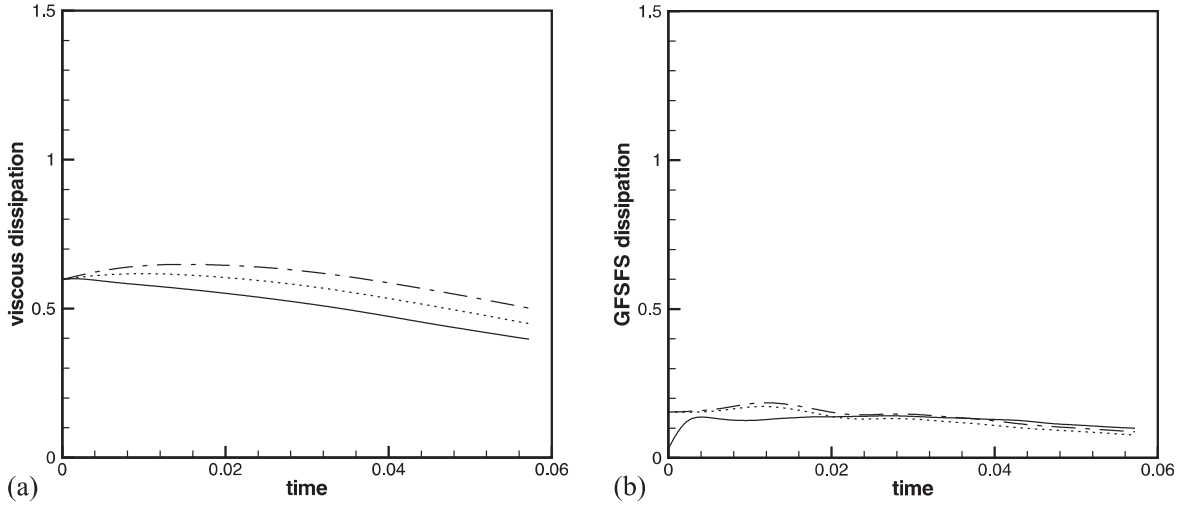

Fig. 9a,b. Temporal evolution of the total large-scale viscous (left), $\epsilon^{\nu}_{r,\mathrm{tot}}$, and GFSFS dissipation (right), $\epsilon^{\mathrm{GFSFS}}_{\mathrm{tot}}$, for the LES solution with mixed models: filtered *Bardina* (— · —) and filtered *Leonard* (· · · · · ·) models plus dynamic Smagorinsky model compared to the doubly filtered DNS (——)

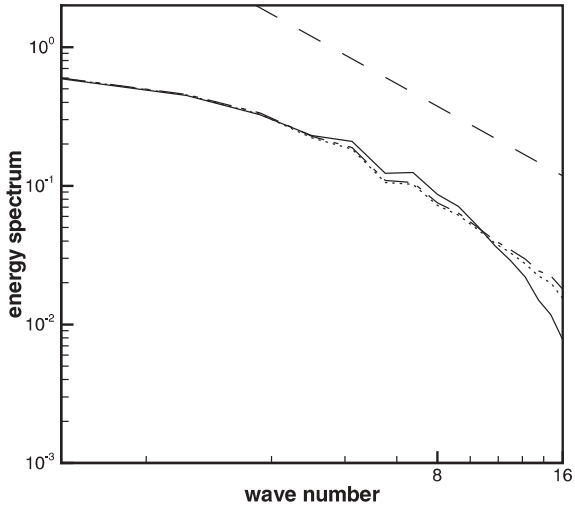

Fig. 10. Density energy spectra for LES solutions with filtered *Bardina* (— · —) and filtered *Leonard* (· · · · · ·) models plus dynamic Smagorinsky model compared to the doubly filtered DNS (——) for $t - t_0 = 0.5\tau_{\mathrm{eddy}}$

5 Conclusions

The LES formulation is inherent to the application of numerical methods with a resolution not sufficient to solve for all the scales of turbulence. For finite difference methods, low resolution not only reduces the range of the flow scales that are effectively resolved (thus acting as an implicit sharp cutoff filter), but also has a smoothing effect on the resolved scales. The classical viewpoint that *large* and *small* stand for *resolved* and *unresolved* scales is actually not valid. In fact, even when a clear separation of scales is introduced by explicitly treating the NS equations by means of a sharp Fourier cutoff filter, the large-scale motions remain partly unresolved by virtue of implicit smooth grid filtering. This effect can be very strong, especially for lower order finite difference methods. The closure model introduced to simulate residual stresses must be consistent with the filter effectively employed in the simulation and, thus, it should also rely on the numerical method itself. In fact, an efficient SGS model should be able to reproduce the effects of the loss of information at large scale level due to the adopted numerics. This makes it particularly difficult to develop good SGS models, since the effective shape of the implicit filter can not be defined.

An analytical filter, namely the tensorial product of 1-D box filters along each spatial direction, was used as an example of smooth filter. The effect of filtering was studied using the *perfect* modeling approach. It was demonstrated that the ideal reference solution for LES verification should be consistent with the filter shape regardless of employed SGS model.

The performances of different classical SGS models were examined using the *perfect* modeling approach in partly modeling large- and small-scale contributions. It was verified that the use of mixed models is unavoidable when solving doubly filtered NS equations. Bardina scale-similarity and/or Leonard-like models are necessary to reconstruct large-scale contributions. Nevertheless, these models do not provide proper dissipation and they must be supplemented by eddy-viscosity models. Several mixed models were analyzed and the mixed Leonard-Smagorinsky model showed good results. Note that the present SGS modeling analysis was not conducted by means of a priori tests, as usually is done in similar studies, since the model performance was effectively evaluated during the simulation.

It is worth noting that one way to avoid the effect of implicit filtering is to use high order numerical methods, together with explicit truncation of the smallest resolved scales. However, this is only partially effective, since the use of a mesh size much smaller than the primary filter width is prohibitively expensive. In fact, just considering a numerical mesh two times finer than the filter width, the cost increases by a factor of eight on a three-dimensional mesh. However, this may be a fair price to pay for doing well-controlled and well-understood LES. In simulating turbulent flows of engineering and scientific interest, one would like to optimize the use of available computer resources by reducing the cost of explicit filtering or avoiding it at all. Thus, the development of efficient models for the additional residual stresses induced by the grid filtering still remains a fundamental issue in LES research.

Acknowledgments. The first author (G. De Stefano), was partially supported by the *Italian National Research Council* (CNR), program *Agenzia 2000* under grant No. CNRG008B87. This support is gratefully acknowledged. Partial support for the second author (O.V. Vasilyev) was provided by the National Science Foundation (NSF) under grants No. EAR-0242591, EAR-0327269 and ACI-0242457 and National Aeronautics and Space Administration (NASA) under grant No. NAG-1-02116.

References

1. Bardina, J., Ferziger, J.H., Reynolds, W.C.: Improved turbulence models based on large eddy simulation of homogeneous incompressible turbulence. Ph.D. Thesis, *Report TF-19*. Thermosciences Div., Dept. of Mech. Eng., Stanford University (1983)
2. Carati, D., Winckelmans, G.S., Jeanmart, H.: On the modelling of the subgrid-scale and filtered-scale stress tensors in large-eddy simulation. J. Fluid Mech. **441**, 119–138 (2001)
3. Chow, F.K., Moin, P.: A further study of numerical errors in large-eddy simulations. J. Comp. Phys. **184**, 366–380 (2003)
4. De Stefano, G., Vasilyev, O.V.: Sharp Cutoff versus Smooth Filtering in Large Eddy Simulation. Phys. Fluids **14**(1), 362–369 (2002)
5. Deardorff, J.W.: A numerical study of three-dimensional turbulent channel flow at large Reynolds numbers. J. Fluid Mech. **41**, 453–480 (1970)
6. Domaradzki, J.A., Saiki, E.M.: A subgrid-scale model based on the estimation of unresolved scales of turbulence. Phys. Fluids **9**(7), 2148–2164 (1997)
7. Eswaran, V., Pope, S.B.: Direct numerical simulations of the turbulent mixing of a passive scalar. Phys. Fluids **31**, 506 (1988a)
8. Eswaran, V., Pope, S.B.: An examination of forcing in direct numerical simulations of turbulence. Comput. Fluids **16**, 257 (1988b)
9. Germano, M., Piomelli, U., Moin, P., Cabot, W.H.: A dynamic subgrid-scale eddy viscosity model. Phys. Fluids A **3**(7), 1760–1765 (1991)
10. Geurts, B.J.: Inverse modeling for large eddy simulation. Phys. Fluids **9**(12), 3585–3587 (1997)
11. Geurts, B.J., Frolich, J.: A framework for predicting accuracy limitations in large eddy simulation. Phys. Fluids **14**(16), L41–L44 (2002)
12. Ghosal, S.: An analysis of numerical errors in large eddy simulations of turbulence. J. Comp. Phys. **125**, 187–206 (1996)
13. Gullbrand, J., Chow, F.K.: Investigation of numerical errors, subfilter-scale models, and subgrid-scale models in turbulent channel flow simulations. In: *Proceeding of the Summer Program*. Center for Turbulence Research, NASA Ames/Stanford University, USA, pp. 87–104 (2002)
14. Jeanmart, H., Winckelmans, G.S.: Comparison of recent dynamic subgrid-scale models in turbulent channel flow. In: *Proceeding of the Summer Program*. Center for Turbulence Research, NASA Ames/Stanford University, USA, pp. 105–116 (2002)

15. Jimenez, J.: *On why dynamic subgrid-scale models work*. Center for Turbulence Research Annual Research Briefs, pp. 25–34 (1995)
16. Leonard, A.: Energy cascade in large-eddy simulations of turbulent fluid flows. Adv. Geophys. **18**, 237–248 (1974)
17. Leonard, A.: Large-eddy simulation of chaotic convection and beyond. In: *Proceedings of 35th Aerospaces Sciences Meeting & Exhibit*, AIAA Paper 97-0204, pp. 93–104 (1997)
18. Lilly, D.K.: A proposed modification of the Germano subgrid-scale closure method. Phys. Fluids **4**, 633–635 (1992)
19. Lund, T.S.: On the use of discrete filters for large eddy simulation. *Center for Turbulence Research Annual Research Briefs*. pp. 83–95 (1997)
20. Lund, T.S., Kaltenbach, H.-J.: Experiments with explicit filtering for LES using a finite-difference method. *Center for Turbulence Research Annual Research Briefs*. pp. 91–105 (1995)
21. Meneveau, C., Katz, J.: Scale-invariance and turbulence models for large-eddy simulation. Annu. Rev. Fluid Mech. 1–32 (2000)
22. Meyers, J., Geurts, B.J., Baelmans, M.: Database analysis of errors in large eddy simulation. Phys. Fluids **15**(9), 2740–2755 (2003)
23. Piomelli, U., Moin, P., Ferziger, J.H.: Model consistency in large eddy simulation of turbulent channel flows. Phys. Fluids **7**, 1884–1891 (1988)
24. Rogallo, R.S., Moin, P.: Numerical simulation of turbulent flow. Ann. Rev. Fluid Mech. **16**, 99–137 (1984)
25. Ruetsch, G.R., Maxey, M.R.: Small-scale features of the vorticity and passive scalar fields in homogeneous isotropic turbulence. Phys. Fluids **3**, 1587–1597 (1991)
26. Schumann, U.: Subgrid scale model for finite difference simualtions of turbulent flows in plane channels and annuli. J. Comp. Phys. **18**, 376–404 (1975)
27. Smagorinsky, J.S.: General circulation experiments with the primitive equations. Mon. Weather Rev. **91**, 99–164 (1963)
28. Stoltz, S., Adams, N.: An approximate deconvolution precedure for large-eddy simulation. Phys. Fluids **11**, 1699–1701 (1999)
29. Vasilyev, O.V., Lund, T.S., Moin, P.: A general class of commutative filters for LES in complex geometries. J. Comp. Phys. **146**, 105–123 (1998)
30. Vreman, B., Geurts, B., Kuerten, H.: Large-eddy simulation of the temporal mixing layer using the mixed Clark model. Theoret. Comput. Fluid Dynamics **8**, 309–324 (1996)
31. Winckelmans, G.S., Wray, A.A., Vasilyev, O.V.: Testing of a new mixed model for LES: the Leonard model supplemented by a dynamic Smagorinsky term. In: *Proceeding of the Summer Program*. Center for Turbulence Research, NASA Ames/Stanford University, USA, pp. 367–388 (1998)
32. Winckelmans, G.S., Wray, A.A., Vasilyev, O.V., Jeanmart, H.: Explicit-filtering large-eddy simulation using the tensor-diffusivity model supplemented by a dynamic Smagorinsky Term. Phys. Fluids **13**(5), 1385–1403 (2001)